

# UCLA

## UCLA Previously Published Works

### Title

Membrane Proteins Can Have High Kinetic Stability

### Permalink

<https://escholarship.org/uc/item/12b2w2p2>

### Journal

Journal of the American Chemical Society, 135(40)

### ISSN

0002-7863

### Authors

Jefferson, Robert E

Blois, Tracy M

Bowie, James U

### Publication Date

2013-10-09

### DOI

10.1021/ja407232b

Peer reviewed



Published in final edited form as:

*J Am Chem Soc.* 2013 October 9; 135(40): . doi:10.1021/ja407232b.

## Membrane proteins can have high kinetic stability

Robert E. Jefferson<sup>†</sup>, Tracy M. Blois<sup>†,‡</sup>, and James U. Bowie<sup>\*,†</sup>

<sup>†</sup>Department of Chemistry and Biochemistry, University of California, Los Angeles-Department of Energy Institute for Genomics and Proteomics, Molecular Biology Institute, University of California, Los Angeles, CA 90095, United States

### Abstract

Approximately 10% of water soluble proteins are considered kinetically stable with unfolding half-lives in the range of weeks to millenia. These proteins only rarely sample the unfolded state and may never unfold on their respective biological timescales. It is still not known whether membrane proteins can be kinetically stable, however. Here we examine the subunit dissociation rate of the trimeric membrane enzyme diacylglycerol kinase from *Escherichia coli* as a proxy for complete unfolding. We find that dissociation occurs with a half-life of at least several weeks, demonstrating that membrane proteins can remain locked in a folded state for long periods of time. These results reveal that evolution can use kinetic stability to regulate the biological function of membrane proteins, as it can for soluble proteins. Moreover, it appears that the generation of kinetic stability could be a viable target for membrane protein engineering efforts.

### Introduction

Some proteins unfold extremely slowly. Wilfredo Colon's lab has identified a large collection of kinetically stable proteins by looking for resistance to sodium dodecyl sulfate (SDS) denaturation. These proteins unfold with apparent half-lives ranging from 79 days to 346 years.<sup>1,2</sup> Pilus protein complexes may have the record for slow unfolding with an estimated half-life of 3 billion years.<sup>3</sup> Most kinetically stable proteins are also thermodynamically stable, but not always. For example, folding of  $\alpha$ -lytic protease is catalyzed and driven by a pro-region. Once the pro-region is cleaved off, the enzyme is thermodynamically unstable, but remains locked in the folded state because the unfolding half-life is about 1.2 years.<sup>4</sup> Characteristics of kinetically stable water-soluble proteins include a high degree of rigidity, considerable beta sheet structure, and a dearth of monomers.<sup>1,2</sup>

It remains unknown whether the different folding energetics or topology restrictions in the membrane could allow for high kinetic stability. It is particularly questionable for  $\alpha$ -helical membrane proteins since almost all the known kinetically stable proteins contain  $\beta$ -sheets, perhaps because of their high contact order<sup>1</sup>. Indeed, the best indication of kinetic stability in membrane proteins comes from unfolding rate studies of the  $\alpha$ -barrel porin PagP.<sup>5</sup> For this protein, unfolding rates could be measured at urea concentrations above 8.5 M.

\*Corresponding Author: Department of Chemistry & Biochemistry, UCLA, Boyer Hall, 611 Charles E. Young Dr. E., Los Angeles, CA 90095-1570. Tel: 310-206-4747. E-mail: bowie@mbi.ucla.edu.

<sup>‡</sup>Present Addresses: Amgen, One Amgen Center Drive, 28-5-B, Thousand Oaks, CA 91320-1799

**Supporting Information.** Supporting Figures 1 and 2. This material is available free of charge via the Internet at <http://pubs.acs.org>.

**Author Contributions:** The manuscript was written through contributions of all authors. All authors have given approval to the final version of the manuscript.

**Notes:** The authors declare no competing financial interest.

Extrapolation back to zero denaturant predicts an unfolding half-life for PagP of more than half a year. Whether the long extrapolation is valid is unclear, however.

There are some indications that helical membrane proteins can be kinetically stable. Yinan Wei's lab found that upon mixing or co-expression of distinguishable subunits of the trimeric membrane protein AcrB, a non-equilibrium distribution is found.<sup>6</sup> This suggests that the oligomers must not exchange completely over the hours needed to express and analyze them. Subunit exchange of dimeric EmrE was also found to take many hours under native conditions.<sup>7</sup> Even the simple glycoporphin A transmembrane helix dimer is known to require hours to exchange in certain detergents.<sup>8</sup> A number of membrane proteins have been found to be resistant to SDS denaturation<sup>9-15</sup> and by analogy with Wilfredo Colon's experiments on soluble proteins, this might reflect high kinetic stability. On the other hand, it might also simply indicate high thermodynamic stability as the denaturing power of SDS is likely to be much greater for soluble proteins than membrane proteins, which are already coated by a band of detergent. Extrapolation of SDS-driven unfolding of bacteriorhodopsin to zero SDS suggest a remarkable unfolding half-life of ~20 million years,<sup>16</sup> but extrapolations for SDS unfolding rates are particularly uncertain.

Given the doubts inherent in extrapolating from high denaturant concentrations, it would be ideal to examine unfolding rates under native conditions. To this end, we examined the subunit dissociation kinetics of diacylglycerol kinase (DGK) from *Escherichia coli* as a proxy for unfolding rate. DGK is an obligate trimer with three transmembrane and one amphipathic helix per subunit. A recent crystal structure of the enzyme reveals a structure in which the nine transmembrane helices of the trimer are closely packed around a central axis (Figure 1A).<sup>17</sup> An earlier NMR structure showed a domain-swapped architecture in which the C-terminal transmembrane helix shifts over to an adjacent subunit.<sup>18</sup> It seems clear that the crystal structure is a fully active enzyme, but it is not known if the domain-swapped form can also be active. Subunit mixing experiments<sup>19</sup> and both structures show that the three active sites are shared between subunits. Thus, a monomer is necessarily inactive.

We posit that subunit dissociation must either precede or be concomitant with complete unfolding. In particular, if the subunits can remain folded as monomers, then dissociation precedes unfolding and the dissociation rate reports an upper limit of the unfolding rate. If local unfolding can occur within the intact oligomer, then the rate of subunit dissociation reports the rate of unfolding of a folded oligomeric core so that subunit dissociation is concomitant with complete unfolding. Thus, the dissociation rate provides an upper bound on the overall unfolding rate.

To examine dissociation/unfolding rates under native conditions we took two approaches: steric trapping and subunit exchange measurements. We find that subunit dissociation can be extremely slow, on the order of weeks for DGK, consistent with high kinetic stability of the trimer.

## Materials and Methods

### Materials

The pQE80 vector and Ni-NTA resin were obtained from QIAGEN (Valencia, CA). Anagrade n-octyl- $\beta$ -D-glucopyranoside (OG) and isopropyl- $\beta$ -D-thiogalactopyranoside (IPTG) were purchased from Affymetrix (Santa Clara, CA). *E. coli* polar lipid extract was purchased from Avanti Polar Lipids, Inc. (Alabaster, AL). N-(3-propionylmaleimidyl)biocytin (BM) was purchased from Life Technologies (Grand Island, NY).

## Cloning, Expression, and Purification of proteins

The natural Cys residues in the DGK expression plasmid pSD005<sup>20</sup> were changed to Ala using site-directed mutagenesis (QuikChange, Agilent) to create a cysless His<sub>6</sub>-DGK construct (DGK<sub>Cysless</sub>). Ile 53 of DGK<sub>Cysless</sub> was mutated to Cys to create the single-cysteine mutant DGK<sub>Cysless/I53C</sub>. Five glutamate residues were added to DGK<sub>Cysless</sub> by inserting the sequence, 5'-CGAAGAAGAAGAAGAAGAGCT-3', at the SacI site (ELEEEEE) following the N-terminal His<sub>6</sub>-tag to create E<sub>5</sub>-DGK<sub>Cysless</sub>. DGK<sub>Cysless</sub>, DGK<sub>Cysless/I53C</sub> and E<sub>5</sub>-DGK<sub>Cysless</sub> were expressed in WH1061 cells at 37 °C for 3 h after induction with 1 mM IPTG.

For the coexpression of cysless and charged DGK, the genes were sub-cloned into pQE80 and pBAD/HisA/p15A<sup>21</sup>, respectively. Each vector was modified by insertion of a SpeI site (ACTAGT) after the start codon by site-directed mutagenesis. The His<sub>6</sub>-tag coding region of pQE80 was replaced with ACTAGT to give pQE80/SpeI. Insertion of DGK<sub>Cysless</sub> using SpeI and HindIII restriction sites added residues MRGSTS to the N-terminus of the pSD005 construct to give pQ-DGK<sub>Cysless</sub>. ACTAGT was inserted after the fourth encoded amino acid of pBAD/HisA/p15A just before the His<sub>6</sub> tag to give pBAD/HisA/p15A/SpeI. Insertion of E<sub>5</sub>-DGK<sub>Cysless</sub> using SpeI and HindIII restriction sites added residues MGGSTS to the N-terminus of the pSD005 construct to give pB-E<sub>5</sub>-DGK<sub>Cysless</sub>. pQ-DGK<sub>Cysless</sub> and pB-E<sub>5</sub>-DGK<sub>Cysless</sub> were coexpressed in TOP10 cells at 18 °C overnight after induction with 0.1 mM IPTG and 0.2% arabinose. All DGK proteins were purified in 1.5% OG as previously described.<sup>22</sup>

DGK<sub>E76L</sub> was created by site-directed mutagenesis of the wild-type DGK in pSD005. To prepare for refolding experiments, DGK<sub>E76L</sub> purified in 1.5% OG was passed through an Econo-Pac 10DG desalting column (Bio-Rad, Hercules, CA) that had been previously equilibrated with SDS unfolding buffer (50 mM NaPO<sub>4</sub> (pH 7.5), 50 mM NaCl, 1% SDS). The peak fraction was diluted to 40 μM with SDS unfolding buffer, snap frozen in liquid nitrogen and stored at -80 °C.

Monovalent streptavidin variants containing one active subunit per streptavidin tetramer were prepared as described previously.<sup>23</sup>

## Chemical biotinylation of DGK

Biotin labeling was performed by incubating 162 μM DGK<sub>Cysless/I53C</sub> in 50 mM NaPO<sub>4</sub> (pH 7.5), 50 mM NaCl, 1.5% OG, 1 mM TCEP with the addition of solid BM to a final concentration of 9 mM. Samples were incubated for 1 h at room temperature followed by 2 h at 4 °C. Labeling reactions were centrifuged at 14,000 × g for 10 min to remove any undissolved label and the supernatant was applied to 400 μL of Ni-NTA resin. Biotinylated DGK (BM-DGK<sub>Cysless/I53C</sub>) samples were incubated with the resin for 1.5 h at 4 °C and then washed with 30 mM imidazole in 50 mM NaPO<sub>4</sub> (pH 7.5), 300 mM NaCl, 1.5% OG, 5 mM -ME and eluted with 300 mM imidazole in the same buffer. All elution fractions were pooled and then dialyzed against 250 mL 50 mM NaPO<sub>4</sub> (pH 7.5), 50mM NaCl, 1.5% OG, 1 mM TCEP. Labeled samples were flash frozen in small aliquots using liquid nitrogen, and stored at -80 °C. A fresh aliquot was used for all subsequent experiments. Labeling was confirmed by mass spectrometry analysis. Samples were co-precipitated with matrix on a stainless steel MALDI plate (Life Technologies) in a 1:1 (v:v) ratio of protein sample to sinapinic acid matrix solution (saturated solution in 50% acetonitrile, 0.1% trifluoroacetic acid). The dried spot was desalted by washing with 1 μL of water three times. 1 μL of sinapinic acid matrix solution was added to the spot and allowed to dry before acquiring MALDI-MS data on a Voyager DE-STR time-of-flight (TOF) mass spectrometer (Applied

Biosystems, Foster City, CA). Mass spectra were collected in linear mode with 1000 shots per spectrum. Spectra were processed using Voyager Data Explorer (Applied Biosystems).

### DGK steric trap assays

BM-DGK<sub>Cysless/I53C</sub> was incubated in 10-fold molar excess mSA or 20-fold molar excess mSA<sub>S45A</sub> at room temperature in DGK incubation buffer (50 mM NaPO<sub>4</sub> (pH 7.5), 50 mM NaCl, 1.5% OG) with 0.2 X<sub>SDS</sub> (calculated from total bulk concentrations of OG and SDS). To equilibrate DGK and mSA in 0.2 X<sub>SDS</sub> before steric trapping, the proteins were equilibrated in separate tubes in DGK incubation buffer with 0.2 X<sub>SDS</sub> for up to 2 h at room temperature. The mSA stock solution in 20 mM NaPO<sub>4</sub> (pH 7.0) was diluted with 5x DGK incubation buffer with 1.85% SDS, and then added to DGK after equilibration. At increasing time points, 5  $\mu$ L aliquots were removed and assayed for activity by the addition of 45  $\mu$ L of a standard DGK assay mix with either cardiolipin or DMPC as the lipid cofactor as described previously.<sup>22,24</sup> In cases where the DGK concentration was too high to be measured before all the NADH was consumed in the coupled assay, the samples were diluted to 0.2-0.4  $\mu$ M just prior to the assay. Activity at each time point was normalized to activity of a freshly thawed wild-type DGK aliquot in DGK incubation buffer assayed with the same DGK assay mix. Initial activities of BM-DGK<sub>Cysless/I53C</sub> after equilibration in 0.2 X<sub>SDS</sub> were 89-97% as active as the freshly thawed wild-type DGK. Fractional activity was calculated as the fraction of initial normalized activity. Activity plots were fit to either a single or double exponential decay.

For DGK activity recovery experiments after steric trapping, free biotin dissolved in DMSO was diluted 50-fold into aliquots of BM-DGK<sub>Cysless/I53C</sub> samples trapped with a 20-fold molar excess of mSA<sub>S45A</sub> to give a 1000-fold molar excess of free biotin over BM-DGK<sub>Cysless/I53C</sub> subunits. Activity plots for recovered samples were fit to an exponential decay subtracted from the exponential decay of the control sample without mSA.

For reactivation experiments of sterically trapped BM-DGK<sub>Cysless/I53C</sub> in the presence of an excess of inactive mutant subunits, 0.2  $\mu$ M BM-DGK<sub>Cysless/I53C</sub> was first sterically trapped in the presence of 4  $\mu$ M mSA<sub>S45A</sub> for 95 h. 2  $\mu$ L of 40  $\mu$ M SDS-unfolded DGK<sub>E76L</sub> or SDS unfolding buffer was then added to 80  $\mu$ L aliquots of sterically trapped DGK<sub>Cysless/I53C</sub> prior to the addition of 2  $\mu$ L of 8 mM biotin. 5  $\mu$ L of sample was assayed after an additional 3 h incubation at room temperature. For samples with added biotin, mutant, or buffer, activities were multiplied by a scale factor to account for the slight dilution.

### Size-exclusion chromatography binding experiments

Gel filtration of DGK:mSA complexes was performed on a Superdex 200-10/300 column (GE Healthcare Life Sciences, Pittsburgh, PA). The column was equilibrated with DGK incubation buffer for all runs. BM-DGK<sub>Cysless/I53C</sub> trimer was first purified on the same column prior to performing the binding experiment to eliminate protein aggregates. 0.32  $\mu$ M purified BM-DGK<sub>Cysless/I53C</sub> was incubated with 1  $\mu$ M mSA for 30 min at room temperature and free biotin was added to a final concentration of 100  $\mu$ M to prevent any further binding by mSA. 500  $\mu$ L aliquots of 1  $\mu$ M mSA alone, 99  $\mu$ M BM-DGK<sub>Cysless/I53C</sub> alone or the incubated complex were loaded onto the column separately. 500  $\mu$ L fractions were collected and assayed for DGK activity.

### Preparation of proteoliposomes

*E. coli* polar lipid extract dissolved in chloroform was dried in glass tubes under a stream of argon gas and residual solvent was removed by vacuum desiccation for 2 h. 70-144 mg of dried lipids were dissolved in 8 mL of 6% OG in DGK vesicle buffer (20 mM Tris-HCl (pH 8.0), 50 mM NaCl) by vortexing and bath sonication. After solubilization, glycerol was

added to a final concentration of 20% (v/v). 270 nmol of purified DGK<sub>Cysless</sub>, E<sub>5</sub>-DGK<sub>Cysless</sub>, or both was added with 1.5% OG in DGK vesicle buffer to bring the total volume to 16 mL. The mixture was incubated on ice for 30 min before dialysis against DGK vesicle buffer with 20% glycerol over a 24 h period at 4 °C (Spectra/Por 25 kDa cutoff dialysis membrane). After formation of vesicles, the turbid mixture was dialyzed against DGK vesicle buffer to remove glycerol.

The resulting proteoliposomes were purified from aggregated protein by centrifugation over a sucrose cushion. 75% sucrose was added to the proteoliposome samples to a final concentration of 20% and the solution layered over 50% sucrose. The samples were centrifuged at 72,000 × g for 16 h at 4 °C. The turbid top layer of proteoliposomes was removed and diluted 2-fold in DGK vesicle buffer before being pelleted twice at 100,000 × g for 1.5 h at 4 °C. The proteoliposomes were resuspended in 2 mL of DGK vesicle buffer and passed through Nucleopore track-etched membranes (Whatman) with 200 nm pore sizes using a miniextruder (Avanti Polar Lipids) 3-5 times. Extruded proteoliposomes were incubated at room temperature overnight to allow recovery of DGK activity.

### Anion Exchange Chromatography of DGK Trimers

For subunit exchange assays in detergent, 500 µL of 70 µM DGK samples were loaded onto a 1 mL HiTrap Q column (GE Healthcare Life Sciences) pre-equilibrated with 20 mM Tris-HCl (pH 8.0), 1.5% OG. Protein was eluted with an isocratic gradient from 0 to 0.5 M NaCl over 20 mL.

For subunit exchange assays in vesicles, aliquots of proteoliposomes containing DGK<sub>Cysless</sub>, E<sub>5</sub>-DGK<sub>Cysless</sub>, or both were incubated at 37 °C. At each timepoint, aliquots of proteoliposomes containing the same level of DGK activity (activity assayed at t<sub>0</sub>) were solubilized with 4-6% OG in DGK vesicle buffer to a final concentration of 3% OG. Anion exchange chromatography was carried out as in detergent, except the isocratic gradient was extended to 30 mL. 300 µL fractions were collected and assayed for activity.

## Results

### Monitoring DGK dissociation kinetics by steric trapping

To monitor dissociation kinetics, we employed a method called steric trapping.<sup>25-27</sup> The steric trapping concept is outlined in Figure 1. In this approach, we label the protein subunits with biotin at sites that are very close in the folded oligomer. When monovalent streptavidin (mSA) is added to the labeled protein, it can bind to one biotinylated subunit with high affinity, but if the biotin labels are sufficiently close, a second mSA cannot bind due to steric overlap, unless the protein dissociates. When the protein dissociates, an additional mSA can bind, effectively trapping the protein in the dissociated state (Figure 1B).

To apply steric trapping to DGK, we introduced a unique Cys residue, I53C, close to the trimeric axis of symmetry (Figure 1A) into a variant of DGK in which the wild-type Cys residues were removed (DGK<sub>Cysless</sub>). Position 53 was then biotinylated using thiol-reactive N<sup>-</sup>-(3-propionylmaleimidyl) biocytin (BM) to generate BM-DGK<sub>Cysless/I53C</sub>. A MALDI-TOF mass spectrum indicated that ~58% of the subunits contained a single biotin label and ~13% contained two labels due to labeling at a secondary site. Thus, ~71% of the subunits bore a label at position 53. Assuming a perfect binomial distribution of labels, ~80% of the trimers would have 2 or 3 biotin labels at C53 and could be subject to steric trapping. As the active site of DGK is shared between subunits, dissociation upon the addition of mSA can be conveniently monitored by loss of activity.



To investigate the unfolding rate of DGK, mSA was added to BM-DGK<sub>Cysless/I53C</sub> in OG micelles at room temperature. As shown in Figure 2A, BM-DGK<sub>Cysless/I53C</sub> inactivates very slowly (half-life ~12.6 d) in the absence of mSA and the addition of mSA has essentially no effect on the rate of inactivation. When we added 0.2 mole fraction SDS ( $X_{\text{SDS}}$ ), however, the addition of mSA had a dramatic effect on the rate of inactivation (Figure 2B). In the presence of mSA, DGK loses ~60% activity in the first week and then undergoes a slower inactivation phase. The inactivation curve at 0.2  $X_{\text{SDS}}$  in the absence of mSA could be fit to a single exponential with a rate constant of  $k_I = 0.036 \pm 0.001 \text{ d}^{-1}$ . The inactivation curve in the presence of mSA required a double exponential fit with rate constants of  $0.43 \pm 0.05 \text{ d}^{-1}$  (fast phase) and  $0.019 \pm 0.004$  (slow phase). The similar rate constants for the slow phase and  $k_I$  suggest that the slow phase reflects the same inactivation process that occurs in the absence of mSA and that the fast phase reflects inactivation due to steric trapping ( $k_{\text{ST}}$ ).

### Investigating the mechanism of inactivation by steric trapping

The slow rate of inactivation, even in 0.2  $X_{\text{SDS}}$  made an extensive characterization of the mechanism impractical as every experiment requires multiple weeks to perform. Nevertheless, we were able to learn some basic characteristics of the inactivation mechanism. We believe the experiments described below are consistent with the model shown in Figure 1B. In this model, steric trapping causes dissociation primarily to dimers and monomers. The dimers and monomers can reassociate to restore activity, but the rate limiting reassociation/refolding event is a slow unimolecular conformational change. We now present the evidence for this model.

Prior work on the inactivation mechanism at elevated temperatures suggests that the slow irreversible inactivation observed in the absence of mSA reflects a stable, essentially irreversible conformational change that occurs after subunit dissociation.<sup>28</sup> This is consistent with a slowing of the intrinsic inactivation rate as the DGK concentration increases: in the absence of mSA, the intrinsic inactivation rate in 0.2  $X_{\text{SDS}}$  slows from  $k_I = 0.023 \pm 0.004 \text{ d}^{-1}$  at 0.2  $\mu\text{M}$  BM-DGK<sub>Cysless/I53C</sub> to  $k_I = 0.014 \pm 0.003 \text{ d}^{-1}$  at 1.8  $\mu\text{M}$  BM-DGK<sub>Cysless/I53C</sub> (Figure 3, black curves). In this model, the subunits dissociate and then can either reassociate or undergo an irreversible inactivation. In the presence of mSA, however, the subunit dissociation becomes irreversible by steric trapping.

As expected for a unimolecular irreversible dissociation in the presence of mSA, the rate of inactivation by steric trapping is not concentration dependent. Figure 3 shows steric trap inactivation at 0.2  $\mu\text{M}$ , 0.6  $\mu\text{M}$ , and 1.8  $\mu\text{M}$  BM-DGK<sub>Cysless/I53C</sub>. Double exponential fits yield steric trap inactivation rates ( $k_{\text{ST}}$ ) of  $0.4 \pm 0.2 \text{ d}^{-1}$ ,  $0.3 \pm 0.1 \text{ d}^{-1}$ , and  $0.7 \pm 0.2 \text{ d}^{-1}$  for 0.2, 0.6, and 1.8  $\mu\text{M}$  BM-DGK<sub>Cysless/I53C</sub>, respectively. Thus, in spite of a nearly 10-fold change in concentration, there is very little change in steric trap inactivation rates. To test whether mSA binding might be rate limiting, we mixed mSA and BM-DGK<sub>Cysless/I53C</sub>, incubated for 30 min, and then prevented further binding by the addition of excess biotin. Analysis by size-exclusion chromatography indicates that complete binding to the intact trimer occurs within the 30 min incubation (Figure S1) and is therefore too fast to contribute significantly to  $k_{\text{ST}}$ . Overall, these results are consistent with a rate limiting dissociation of a subunit from the trimer or a slow conformational change within the trimer that occurs prior to mSA trapping.

If the sterically trapped state is dissociated, it is possible that the reverse reaction (reassociation) would be concentration dependent, unless a conformational change is rate limiting. We therefore examined the concentration dependence of reactivation after the addition of a biotin competitor. To ensure that the rate of mSA release is fast, we employed a mutant of mSA, mSA<sub>S45A</sub>, with a reduced binding affinity. For this mutant, biotin dissociation occurs with a half-life of less than 2 min at room temperature.<sup>29</sup> As shown in

Figure S2, mSA<sub>S45A</sub> has sufficient binding affinity at the concentrations used to inactivate BM-DGK<sub>Cysless/I53C</sub> to the same extent as mSA. Figure 3 shows the progress of activity recovery after biotin addition (blue traces). Activity recovers slowly over the course of many days, asymptotically approaching the activity decay curve for the enzyme that has not been subject to steric trapping (black traces). We fit these curves to a double exponential reflecting both the recovery of activity  $k_R$  and the slow inactivation of the untrapped enzyme ( $k_I$ , see above). In these fits,  $k_I$  was fixed at the observed inactivation rate in the absence of mSA. At 0.2, 0.6 and 1.8  $\mu\text{M}$  BM-DGK<sub>Cysless/I53C</sub>, we found that  $k_R$  was  $0.20 \pm 0.02$ ,  $0.21 \pm 0.04$ , and  $0.38 \pm 0.07 \text{ d}^{-1}$ , respectively. Thus, activity recovery from the sterically trapped inactive state is only moderately concentration dependent at best. Thus, from the recovery rates alone it is still possible that sterically trapped DGK is not dissociated or there is a rate limiting conformational change at some point during either refolding of the monomers or the trimer that is much slower than the reassociation rate.

To test further whether the subunits are dissociated in the sterically trapped state, we asked whether subunit mixing could occur after steric trap inactivation. The experiment is outlined in the box in Figure 1B. We reasoned that if we added dissociated/unfolded subunits bearing a mutation in one half of the active site, they would be able to freely associate with the sterically trapped monomers and dimers. Reassociation and refolding could then restore complete activity to the sterically trapped subunits, but the mutant subunits would be unable to form active trimers on their own, as illustrated in Figure 1B. For these experiments we first generated a steric trap inactivated BM-DGK<sub>Cysless/I53C</sub> by incubating with mSA<sub>S45A</sub> for 4 days until the activity dropped to about 60% of its starting value (Figure 3A). We then mixed with an inactive mutant of DGK, E76L,<sup>19</sup> which had been previously unfolded at high SDS concentration. If the steric trap inactivated BM-DGK<sub>Cysless/I53C</sub> was dissociated, we expected that the mutant subunits would refold, mix with, and reactivate the BM-DGK<sub>Cysless/I53C</sub> subunits. As shown in Figure 4, we saw essentially complete recovery of activity within 3 hours of mixing with DGK<sub>E76L</sub>. The recovery of activity is considerably faster than reactivation of trapped BM-DGK<sub>Cysless/I53C</sub> without the SDS-unfolded mutant subunits. Fast refolding from an SDS-unfolded state is consistent with earlier work.<sup>30,31</sup> It therefore seems likely that the SDS and steric trap unfolded states are different. Nevertheless, the SDS unfolded subunits are capable of refolding with the sterically trapped form and restore activity, indicating that the steric trap inactivated protein is dissociated.

While the results are consistent with the basic model outlined in Figure 1B, in a system this complex, we cannot rule out all possible mechanisms or minor parallel pathways for inactivation and reactivation. Nevertheless, we believe that we can make the following key observations: (1) Steric trapping leads to a dissociated or partially dissociated inactive state as expected. (2) The rate of appearance of the dissociated/unfolded state is extremely slow in OG, with a half-life of at least 12.6 d (the rate of inactivation with or without mSA).

### Measuring DGK unfolding by subunit exchange

As an independent measure of subunit dissociation, we examined the kinetics of subunit exchange. We created a subunit that was distinguishable from the wild-type by inserting a pentaglutamate tag at the N-terminus of DGK to create a more negatively charged protein, E<sub>5</sub>-DGK. To prevent the possibility of disulfide bond formation between subunits that could prevent exchange the two native cysteines (C46 and C113) were mutated to alanine to give the constructs used in these experiments: DGK<sub>Cysless</sub> and E<sub>5</sub>-DGK<sub>Cysless</sub>.

As shown in Figure 5A, DGK<sub>Cysless</sub> and E<sub>5</sub>-DGK<sub>Cysless</sub> can be clearly separated on an ion exchange column. When the two distinct subunits are expressed together in the same cell, we observe mixed subunit compositions, although the distribution is biased toward DGK<sub>Cysless</sub>, which expresses at higher levels than E<sub>5</sub>-DGK<sub>Cysless</sub>. To monitor subunit



exchange rates, we incubated an equimolar mixture of DGK<sub>Cysless</sub> and E<sub>5</sub>-DGK<sub>Cysless</sub> at room temperature in OG and monitored subunit exchange by separation on the anion exchange column. Very little exchange occurred even after 7 days of incubation (Figure 5B). Moreover, as shown in Figure 5C, ~86% of the activity is maintained after 2 days and ~72% after 7 days. Thus, the lack of subunit exchange cannot be explained by rapid irreversible dissociation of subunits. The final ratio of the mixed peaks to the pure DGK<sub>Cysless</sub> or E<sub>5</sub>-DGK<sub>Cysless</sub> peaks is expected to be 3:1 based on binomial sorting, yet the ratio is only ~0.3 after 7 days, indicating that subunit exchange has only progressed to about 10% of its expected final value. These results imply that the half-life of subunit exchange in OG is at least ~5 weeks.

To compare our experiments in detergent micelles to more physiologically relevant conditions, we measured DGK subunit exchange in vesicles made from *E. coli* lipids. Proteoliposomes containing DGK<sub>Cysless</sub>, E<sub>5</sub>-DGK<sub>Cysless</sub>, or a mixture of both in the same vesicles were prepared and incubated at 37 °C (Figure 6). After incubation, the vesicles were solubilized in OG (where only slow exchange occurs) and the subunit distributions analyzed by anion exchange chromatography as before. It was necessary to use smaller quantities of enzyme for the vesicle experiments, so we detected DGK by activity measurements rather than absorbance at 280 nm. The results of these incubations are shown in Figure 6. The activities and subunit compositions remain largely unchanged over the 2 d incubation period at 37 °C. Longer incubations were not attempted because loss of liposome integrity can be significant after many days.<sup>32</sup> Nevertheless, it is clear that subunit exchange is very slow under physiological conditions, as we found for the detergent-solubilized enzyme.

## Discussion

Our results indicate that subunit dissociation of DGK is extremely slow. Under the destabilizing conditions of 0.2 X<sub>SDS</sub>, subunit dissociation occurs with a half-life of about 1.6 d as measured by the steric trap inactivation rate ( $k_{ST}$ ). In the absence of steric trapping, the protein inactivates much more slowly and the rate of inactivation is slowed by increased concentration. Previous work on the inactivation mechanism at elevated temperatures also found a protection effect at higher concentration.<sup>28</sup> As suggested previously, we believe this must reflect a partially reversible dissociation step that occurs prior to inactivation of the dissociated subunit. Steric trapping renders this partially reversible dissociation completely irreversible. In pure OG without SDS, steric trapping does not enhance the rate of inactivation. This suggests that dissociation is largely irreversible under these conditions rendering the inactivation rate with and without mSA the same. It should be noted that OG solubilization can also be considered partially destabilizing conditions because the enzyme is more stable in other, longer chain detergents.<sup>20</sup> Nevertheless, the inactivation/dissociation rate in OG is very slow, on the order of 2 weeks (12.6 d).

As an independent measure of subunit dissociation rates, we also examined the rate of subunit exchange. Only ~10% subunit exchange was observed over the course of seven days in OG, and no subunit exchange was observed after 2 days under physiological conditions of *E. coli* lipid vesicles at 37 °C. Thus, on the time scale of an *E. coli* cell with a doubling time of ~30 min, DGK essentially never dissociates.

Although the proximity of residue 53 in the trimer can permit crosslinking of subunits in the I53C mutant in the presence of oxidizing agents<sup>34</sup>, the slow dissociation observed here cannot be due to disulfide bonding. Steric trap inactivation requires multiple labels, precluding disulfide formation in proteins that are subject to the effects of steric trapping. Moreover, we saw no evidence for dimer formation in mass spectra of either the unlabeled or BM-labeled proteins, consistent with the high percentage of labeling observed (~71%).

Disulfide formation was not possible in the subunit mixing experiments since they were performed on a cysless variant of DGK.

How might this high kinetic stability be achieved? A likely mechanism is high thermodynamic stability. As yet, there are no measurements for the thermodynamic stability of helical membrane proteins under native conditions that do not involve an uncertain extrapolation from high denaturant concentrations. Nevertheless, theoretical arguments from Deeds *et al* suggest that cyclic oligomers should be particularly stable.<sup>35</sup> In the simple case of a cyclic trimer, formation of a dimer must be sufficiently stable to overcome the entropy cost of reducing two freely diffusing protein subunits to a single complex. The completion of the trimer involves the same entropic cost term, but the stabilizing contribution from the interface is doubled because the final subunit forms two interfaces instead of just one, providing a high level of stability. Cyclic oligomers are a natural symmetry for membrane proteins that are constrained to a planar bilayer. Indeed, AcrB is a cyclic trimer and appears to also have a slow subunit dissociation rate.<sup>6</sup> As kinetic stability is likely to be a favorable property for biochemical and structural studies of membrane proteins, it might therefore make sense to look for membrane protein homologs that are higher order oligomers.

In the cell, proteins are often degraded by proteases that recognize unfolded segments. Proteins that do not often sample the unfolded state are resistant to proteolysis,<sup>36</sup> and thus would require some active mechanism of degradation. In *E. coli*, the membrane-bound AAA protease FtsH is known to degrade an unstable mutant of DGK, but not wild-type DGK.<sup>37</sup> It may also be possible for membrane proteins to be cleaved at sites of local unfolding, which may occur on a faster timescale than the unfolding observed in our experiments. Whether active mechanisms exist or are even needed in *E. coli* to degrade kinetically stable proteins like DGK is unknown.

Evolutionary pressure for high kinetic stability makes sense for an enzyme like  $\beta$ -lytic protease that must operate outside the cell under unforgiving conditions<sup>4</sup>, but the evolutionary advantages membrane protein kinetic stability is less clear. Diacylglycerol kinase plays an important role in generating membrane-derived oligosaccharides that protect cells against osmotic stress conditions.<sup>38</sup> Kinetic stability may therefore be important for a protein that must remain active under harsh conditions. In the milieu of the membrane where there is a high concentration of protein, it may also be advantageous to avoid unfolding that would provide opportunities for inappropriate docking with other transmembrane helices. Helical bundles can have slow rates of folding and unfolding due to frustrated energy landscapes,<sup>39,40</sup> which may also be a feature of transmembrane helices, given the importance of van der Waals packing<sup>41</sup> that could lead to locally stable incorrect conformations. For example Doura and Fleming showed that the transmembrane helix of glycophorin A can dimerize in multiple ways.<sup>42</sup> Differing structures of DGK solved by solution NMR<sup>18</sup> and X-ray crystallography<sup>17</sup> also suggest that it is possible for the helices to pack in stable alternate conformations. Kinetic stability may be a way to protect against the formation of stable, but inactive structures.

How many kinetically stable membrane proteins exist is not clear at this time. It is entirely possible that most of the membrane proteins of known structure are kinetically stable since proteins need to remain folded for the time required to grow crystals or collect NMR spectra. Now that we know that high kinetic stability can be obtained for membrane proteins, a better understanding of the mechanisms of kinetic stability could be of practical importance. It may allow for the engineering of kinetic stability and expand the number of proteins accessible to detailed scrutiny.

## Supplementary Material

Refer to Web version on PubMed Central for supplementary material.

## Acknowledgments

We thank Thomas Magliery (OSU) for insightful discussion, and Bowie lab members for critically reading the manuscript.

**Funding Sources:** This work was supported by NIH grant 5R01GM063919 to JUB and by the Ruth L. Kirschstein National Research Service Award GM007185.

## References

1. Manning M, Colón W. *Biochemistry*. 2004; 43:11248–11254. [PubMed: 15366934]
2. Xia K, Manning M, Hesham H, Lin Q, Bystroff C, Colón W. *Proceedings of the National Academy of Sciences*. 2007; 104:17329–17334.
3. Puorger C, Eidam O, Capitani G, Erilov D, Grütter MG, Glockshuber R. *Structure*. 2008; 16:631–642. [PubMed: 18400183]
4. Jaswal SS, Sohl JL, Davis JH, Agard DA. *Nature*. 2002; 415:343–346. [PubMed: 11797014]
5. Huysmans GHM, Baldwin SA, Brockwell DJ, Radford SE. *Proceedings of the National Academy of Sciences*. 2010; 107:4099–4104.
6. Lu W, Chai Q, Zhong M, Yu L, Fang J, Wang T, Li H, Zhu H, Wei Y. *Journal of Molecular Biology*. 2012; 423:123–134. [PubMed: 22766312]
7. Rotem D, Sal-man N, Schuldiner S. *J Biol Chem*. 2001; 276:48243–48249. [PubMed: 11572877]
8. Fisher LE, Engelman DM, Sturgis JN. *Journal of Molecular Biology*. 1999; 293:639–651. [PubMed: 10543956]
9. Fujii J, Maruyama K, Tada M, MacLennan DH. *J Biol Chem*. 1989; 264:12950–12955. [PubMed: 2502544]
10. Yang B, Gonzalez L, Prekeris R, Steegmaier M, Advani RJ, Scheller RH. *J Biol Chem*. 1999; 274:5649–5653. [PubMed: 10026182]
11. Hardie KR, Lory S, Pugsley AP. *EMBO J*. 1996; 15:978–988. [PubMed: 8605893]
12. Heginbotham L, Odessey E, Miller C. *Biochemistry*. 1997; 36:10335–10342. [PubMed: 9254633]
13. Sargiacomo M, Scherer PE, Tang Z, Kübler E, Song KS, Sanders MC, Lisanti MP. *PNAS*. 1995; 92:9407–9411. [PubMed: 7568142]
14. Borgnia MJ, Kozono D, Calamita G, Maloney PC, Agre P. *Journal of Molecular Biology*. 1999; 291:1169–1179. [PubMed: 10518952]
15. Spelbrink REJ, Kolkman A, Slijper M, Killian JA, Kruijff Bde. *J Biol Chem*. 2005; 280:28742–28748. [PubMed: 15919657]
16. Curnow P, Booth PJ. *Proceedings of the National Academy of Sciences*. 2007; 104:18970–18975.
17. Li D, Lyons JA, Pye VE, Vogeley L, Aragão D, Kenyon CP, Shah STA, Doherty C, Aherne M, Caffrey M. *Nature*. 2013; 497:521–524. [PubMed: 23676677]
18. Van Horn WD, Kim HJ, Ellis CD, Hadziselimovic A, Sulistijo ES, Karra MD, Tian C, Sonnichsen FD, Sanders CR. *Science*. 2009; 324:1726–1729. [PubMed: 19556511]
19. Lau FW, Chen X, Bowie JU. *Biochemistry*. 1999; 38:5521–5527. [PubMed: 10220339]
20. Zhou Y, Bowie JU. *Journal of Biological Chemistry*. 2000; 275:6975–6979. [PubMed: 10702260]
21. Massey-Gendel E, Zhao A, Boulting G, Kim HY, Balamotis MA, Seligman LM, Nakamoto RK, Bowie JU. *Protein Science*. 2009; 18:372–383. [PubMed: 19165721]
22. Lau FW, Bowie JU. *Biochemistry*. 1997; 36:5884–5892. [PubMed: 9153430]
23. Howarth M, Chinnapen DJF, Gerrow K, Dorrestein PC, Grandy MR, Kelleher NL, El-Husseini A, Ting AY. *Nature Methods*. 2006; 3:267–273. [PubMed: 16554831]
24. Badola P, Sanders CR. *J Biol Chem*. 1997; 272:24176–24182. [PubMed: 9305868]

25. Blois TM, Hong H, Kim TH, Bowie JU. *J Am Chem Soc.* 2009; 131:13914–13915. [PubMed: 19739627]
26. Hong H, Blois TM, Cao Z, Bowie JU. *Proceedings of the National Academy of Sciences.* 2010; 107:19802–19807.
27. Hong H, Bowie JU. *J Am Chem Soc.* 2011; 133:11389–11398. [PubMed: 21682279]
28. Zhou Y, Lau FW, Nauli S, Yang D, Bowie JU. *Protein Science.* 2001; 10:378–383. [PubMed: 11266623]
29. Hyre DE, Stayton PS, Trong IL, Freitag S, Stenkamp RE. *Protein Science.* 2000; 9:878–885. [PubMed: 10850797]
30. Nagy JK, Lonzer WL, Sanders CR. *Biochemistry.* 2001; 40:8971–8980. [PubMed: 11467959]
31. Lorch M, Booth PJ. *Journal of Molecular Biology.* 2004; 344:1109–1121. [PubMed: 15544815]
32. Elferink MGL, deWit JG, Driessen AJM, Konings WN. *Biochimica et Biophysica Acta (BBA) - Biomembranes.* 1994; 1193:247–254.
33. Lau FW, Nauli S, Zhou Y, Bowie JU. *Journal of molecular biology.* 1999; 290:559–564. [PubMed: 10390353]
34. Nagy JK, Lau FW, Bowie JU, Sanders CR. *Biochemistry.* 2000; 39:4154–4164. [PubMed: 10747807]
35. Deeds EJ, Bachman JA, Fontana W. *PNAS.* 2012; 109:2348–2353. [PubMed: 22308356]
36. Park C, Zhou S, Gilmore J, Marqusee S. *Journal of Molecular Biology.* 2007; 368:1426–1437. [PubMed: 17400245]
37. Herman C, Prakash S, Lu CZ, Matouschek A, Gross CA. *Molecular cell.* 2003; 11:659–669. [PubMed: 12667449]
38. Van Horn WD, Sanders CR. *Annu Rev Biophys.* 2012; 41:81–101. [PubMed: 22224599]
39. Wensley BG, Batey S, Bone FAC, Chan ZM, Tumelty NR, Steward A, Kwa LG, Borgia A, Clarke J. *Nature.* 2010; 463:685–688. [PubMed: 20130652]
40. Wensley BG, Kwa LG, Shammass SL, Rogers JM, Browning S, Yang Z, Clarke J. *PNAS.* 2012; 109:17795–17799. [PubMed: 22711800]
41. Oberai A, Joh NH, Pettit FK, Bowie JU. *PNAS.* 2009; 106:17747–17750. [PubMed: 19815527]
42. Doura AK, Fleming KG. *Journal of Molecular Biology.* 2004; 343:1487–1497. [PubMed: 15491626]

## Abbreviations

<b>BM</b>	N -(3-propionylmaleimidyl)biocytin
<b>DGK</b>	diacylglycerol kinase
<b>mSA</b>	monovalent streptavidin
<b>OG</b>	n-octyl- -D-glucopyranoside
<b>IPTG</b>	isopropyl- -D-thiogalactopyranoside
<b>MALDI-TOF</b>	matrix-assisted laser desorption ionization time-of-flight
<b>SDS</b>	sodium dodecyl sulfate

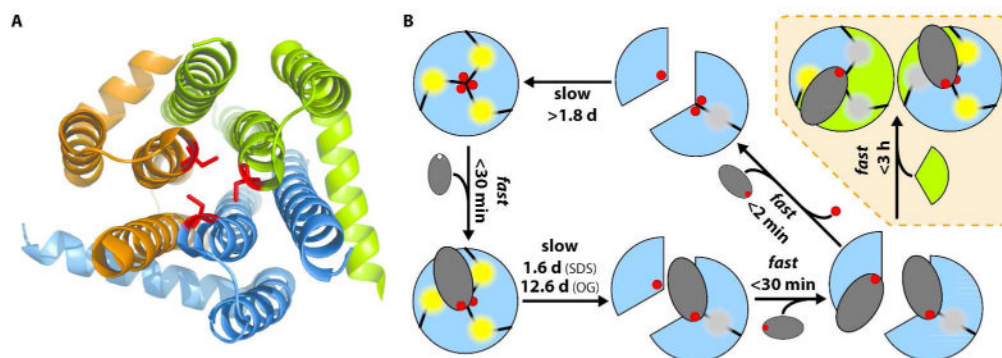


**Figure 1.**

Steric trapping of DGK. (A) Crystal structure of DGK,<sup>17</sup> highlighting the single cysteine introduced at position 53 for biotin labeling. The three distinct subunits are shown in orange, green, and blue. (B) Simple schematic for unfolding and refolding of DGK by the steric trap. The evidence for the reaction scheme investigated in  $0.2 X_{SDS}$  is presented in the text and the results will only be summarized here. The upper left depicts the DGK trimer. The active sites, depicted in yellow, are shared between subunits. The biotin labels are depicted by the red dots. Initial binding of mSA, depicted in dark gray, is unimpeded and can occur rapidly. The binding of a second mSA cannot occur unless the subunits dissociate due to steric overlap with the initially bound mSA. In  $0.2 X_{SDS}$ , the half-life is 1.6 d, while in pure OG, the half-life of dissociation is at least 12.6 d. Once dissociated, a second mSA can bind rapidly, effectively trapping the protein in a dissociated state, hence the term “steric trapping”. If the trapped state is generated with a rapidly dissociating variant of mSA, mSA<sub>S45A</sub>, it can be rapidly removed by the addition of excess free biotin. The dissociated subunits are then free to reassociate. Reassociation is slow, with a half-life of 1.8 d and is not concentration dependent, suggesting a unimolecular conformational change is rate limiting. The conformational change is depicted by a change in shape of the subunits and inactivation of the active sites by the change from yellow to light gray. Evidence for subunit dissociation during steric trapping is provided by the experiment depicted in the shaded box. In this experiment, an unfolded, inactive mutant shown in green was added to a sterically trapped sample. Rapid recovery of activity was observed due to reconstruction of the folded trimers as shown.

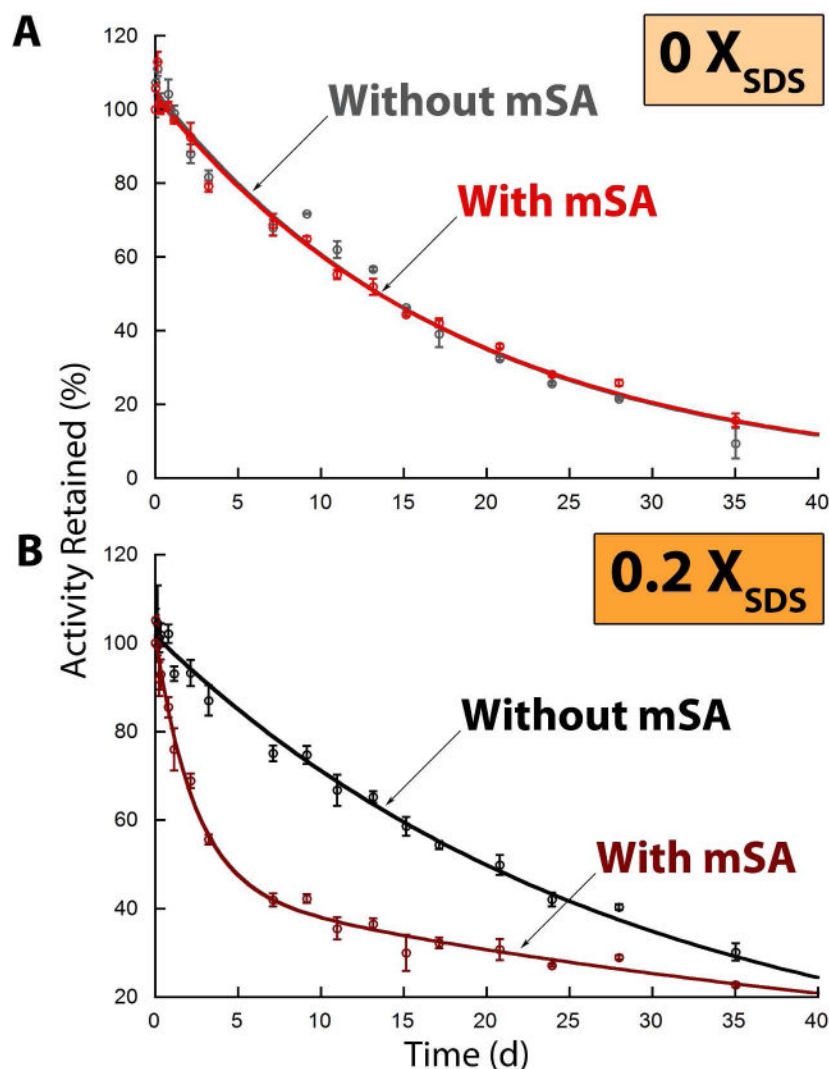


**Figure 2.** DGK inactivation by steric trapping. (A) The results in pure OG (zero SDS). BM-DGK<sub>Cysless/153C</sub> was incubated with (red) or without (gray) mSA. The curves are fits to a single exponential decay. (B) The results in 0.2 X<sub>SDS</sub>. BM-DGK<sub>Cysless/153C</sub> was incubated with (black) or without (dark red) mSA. The curve without mSA is a fit to a single exponential decay. The curve with mSA is a fit to a double exponential decay. Error bars indicate standard deviation of activities measured in triplicate. The specific activity of the enzyme, corresponding to 100% activity, was  $71 \pm 3 \text{ } \mu\text{mol}\cdot\text{min}^{-1}\cdot\text{mg}^{-1}$ , which is within the reported ranges for wild-type DGK<sup>20,24</sup>.



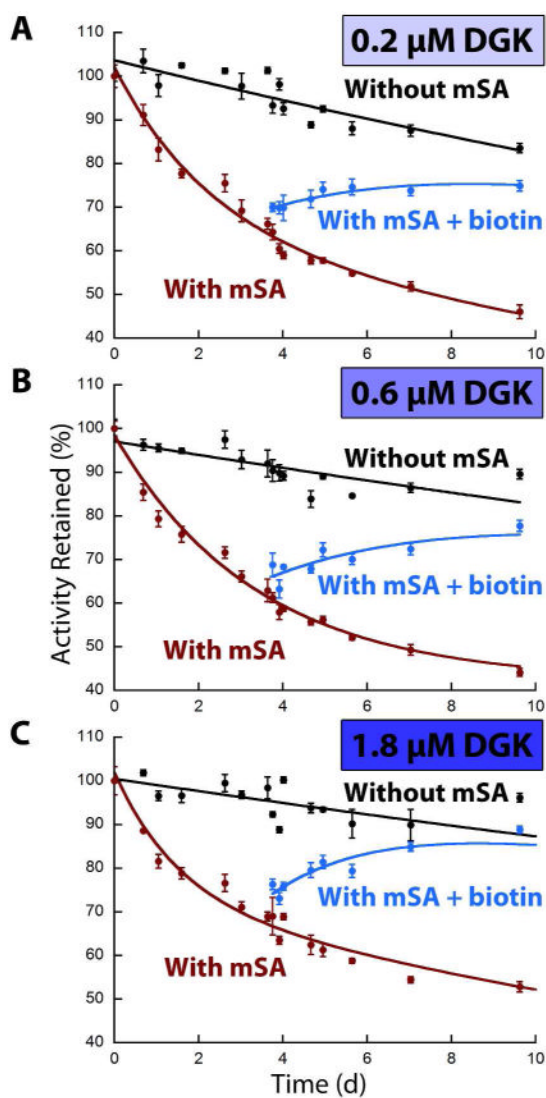


**Figure 3.**

Concentration dependence of steric trap dissociation and reassociation. BM-DGK<sub>Cysless/I53C</sub> was incubated in 0.2 X<sub>SDS</sub> without mSA<sub>S45A</sub> (black) and with mSA<sub>S45A</sub> (red). Free biotin was added to an aliquot of sterically trapped BM-DGK<sub>Cysless/I53C</sub> at 89 h (blue). Data is shown for three different concentrations of BM-DGK<sub>Cysless/I53C</sub>: (A) 0.2 μM (B) 0.6 μM and (C) 1.8 μM. Error bars indicate standard deviation of activities measured in triplicate. The specific activity of the enzyme, corresponding to 100% activity, was  $63 \pm 4$   $\text{umol}\cdot\text{min}^{-1}\cdot\text{mg}^{-1}$ , which is within the reported ranges for wild-type DGK<sup>20,24</sup>.

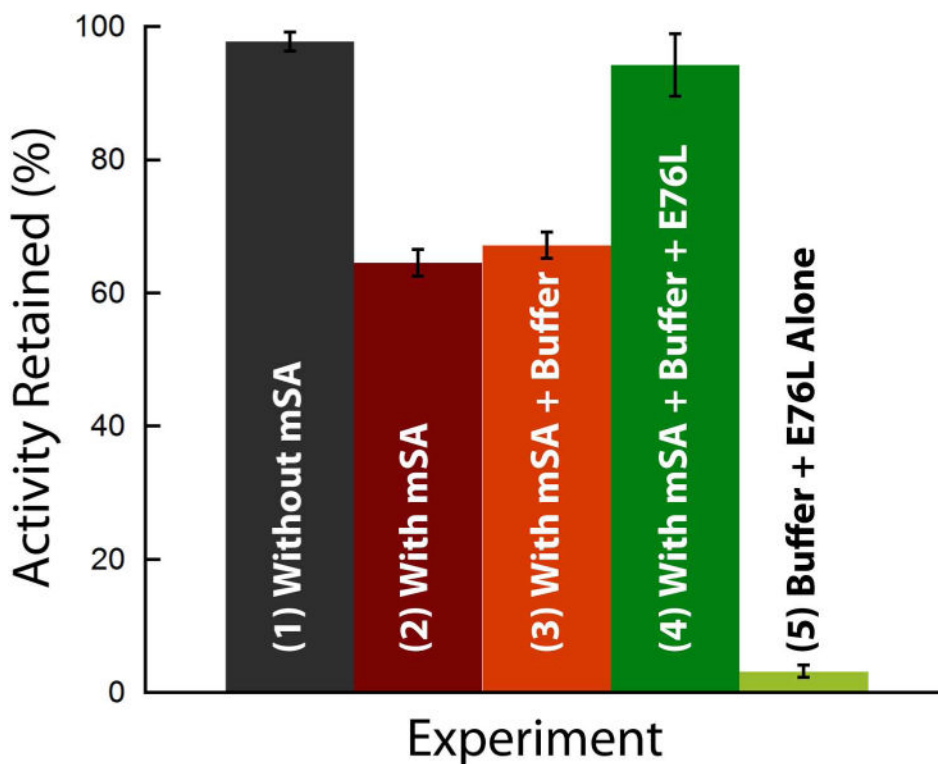


**Figure 4.**

Reactivation of sterically trapped DGK after mixing with the inactive mutant, DGK<sub>E76L</sub>. The experiment is depicted in the shaded box of Figure 1. The relative DGK activities after four different experiments are shown: (1) Incubation of BM-DGK<sub>Cysless/I53C</sub> for 98 h by itself. The activity of this sample is treated as the maximum possible activity that could be recovered. (2) Incubation of BM-DGK<sub>Cysless/I53C</sub> for 98 h in the presence of mSA<sub>S45A</sub> to generate a sterically trapped state. The reduction in activity to ~60% of the value in the absence of mSA indicates the formation of steric trap inactivated enzyme. (3) Addition of the SDS unfolding buffer used to unfold DGK<sub>E76L</sub> by itself to the sterically trapped sample. (4) Addition of a 5-fold molar excess of a previously SDS-unfolded, inactive mutant DGK<sub>E76L</sub> to the sterically trapped sample, followed by further incubation for 3 h. (5) Addition of previously SDS-unfolded DGK<sub>E76L</sub> to the buffer used in steric trapping. Steric trapping was performed in 0.2 X<sub>SDS</sub>. Error bars indicate the standard deviation of activities measured in triplicate.

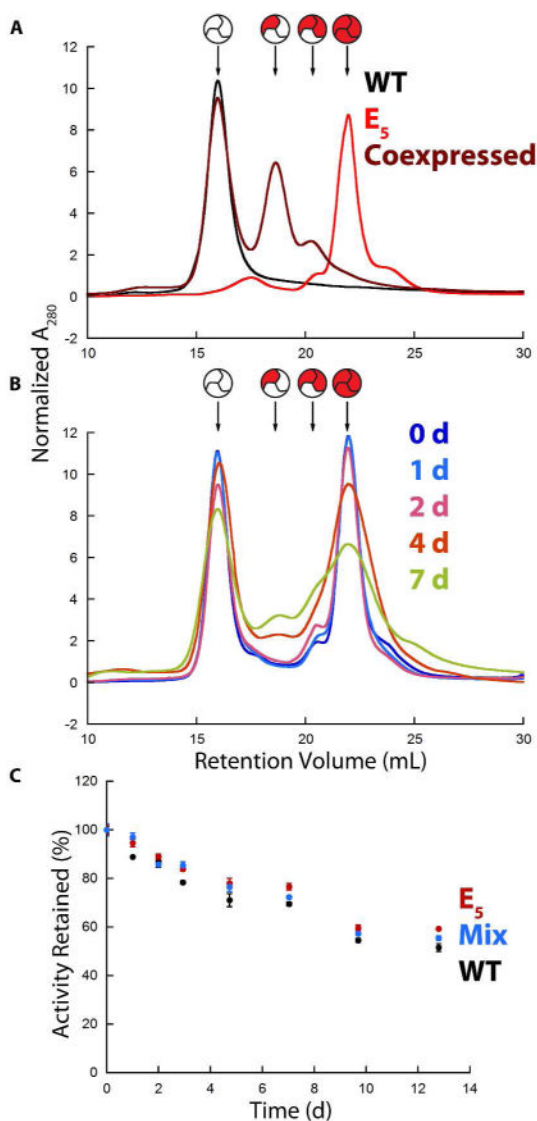


**Figure 5.** Subunit exchange of DGK in 1.5% OG. (A) Anion exchange chromatograms of DGK<sub>Cysless</sub> (black), E<sub>5</sub>-DGK<sub>Cysless</sub> (red), and E<sub>5</sub>-DGK<sub>Cysless</sub> with DGK<sub>Cysless</sub> co-expressed in the same cells (maroon). All samples were maintained at 4 °C during and after purification. (B) Anion exchange chromatograms of DGK<sub>Cysless</sub> and E<sub>5</sub>-DGK<sub>Cysless</sub> that were mixed after purification. The mixed samples were incubated for 0 (blue), 1 (light blue), 2 (pink), 4 (orange), and 7 d (green) at room temperature. Absorbance at 280 nm was normalized to the average value between elution volumes of 10 and 30 mL. (C) Activity (normalized to the initial value) over the time period of the incubation at room temperature. Error bars indicate standard deviation of activities measured in triplicate.

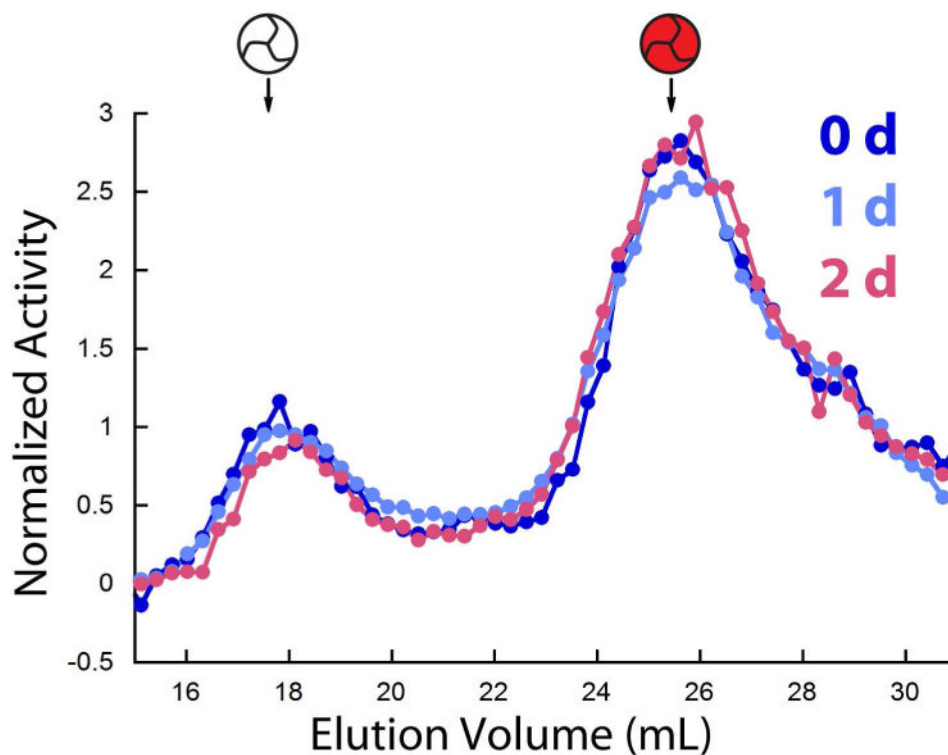


**Figure 6.** Subunit exchange of DGK trimers in *E. coli* polar lipid vesicles. Anion exchange chromatograms are shown of a mix of DGK<sub>Cysless</sub> and E<sub>5</sub>-DGK<sub>Cysless</sub> incubated at 37 °C for 0 (blue), 1 (light blue), and 2 d (pink). Prior to chromatography, the vesicles were solubilized in OG and the chromatography performed in OG buffer. Fractions were assayed for activity and normalized to the average value.